

## Diaminopyridine-Based Potent and Selective Mps1 Kinase Inhibitors Binding to an Unusual Flipped-Peptide Conformation

Ken-ichi Kusakabe,<sup>\*,†</sup> Nobuyuki Ide,<sup>†</sup> Yataro Daigo,<sup>‡,§</sup> Takeshi Itoh,<sup>†</sup> Kenichi Higashino,<sup>†</sup> Yousuke Okano,<sup>†</sup> Genta Tadano,<sup>†</sup> Yuki Tachibana,<sup>†</sup> Yuji Sato,<sup>†</sup> Makiko Inoue,<sup>†</sup> Tooru Wada,<sup>†</sup> Motofumi Iguchi,<sup>†</sup> Takayuki Kanazawa,<sup>†</sup> Yukichi Ishioka,<sup>†</sup> Keiji Dohi,<sup>†</sup> Sachie Tagashira,<sup>†</sup> Yasuto Kido,<sup>†</sup> Shingo Sakamoto,<sup>†</sup> Kazuya Yasuo,<sup>†</sup> Masahiro Maeda,<sup>†</sup> Takahiko Yamamoto,<sup>†</sup> Masayo Higaki,<sup>†</sup> Takeshi Endoh,<sup>†</sup> Kazuo Ueda,<sup>†</sup> Takeshi Shiota,<sup>†</sup> Hitoshi Murai,<sup>†</sup> and Yusuke Nakamura<sup>‡</sup>

<sup>†</sup>Medicinal Research Laboratories, Drug Developmental Research Laboratories, and Innovative Drug Discovery Research Laboratories, Shionogi Pharmaceutical Research Center, 1-1 Futaba-cho 3-chome, Toyonaka, Osaka 561-0825, Japan

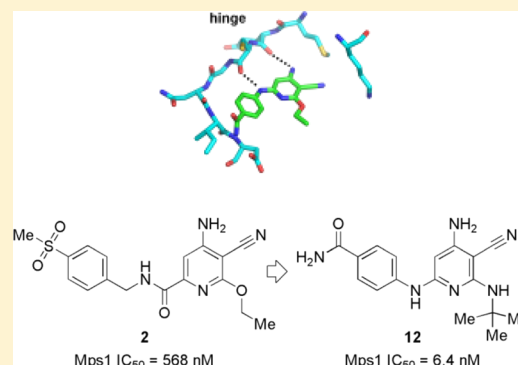
<sup>‡</sup>Laboratory of Molecular Medicine, Human Genome Center, Institute of Medical Science, The University of Tokyo, 4-6-1 Shirokanedai, Minato-ku, Tokyo 108-8639, Japan

<sup>§</sup>Department of Medical Oncology, Shiga University of Medical Science, Seta Tsukinowa-cho, Otsu, Shiga 520-2192, Japan

## S Supporting Information

**ABSTRACT:** Monopolar spindle 1 (Mps1) is an attractive cancer drug target due to the important role that it plays in centrosome duplication, the spindle assembly checkpoint, and the maintenance of chromosomal stability. A design based on JNK inhibitors with an aminopyridine scaffold and subsequent modifications identified diaminopyridine **9** with an  $IC_{50}$  of 37 nM. The X-ray structure of **9** revealed that the Cys604 carbonyl group of the hinge region flips to form a hydrogen bond with the aniline NH group in **9**. Further optimization of **9** led to **12** with improved cellular activity, suitable pharmacokinetic profiles, and good in vivo efficacy in the mouse A549 xenograft model. Moreover, **12** displayed excellent selectivity over 95 kinases, indicating the contribution of its unusual flipped-peptide conformation to its selectivity.

**KEYWORDS:** monopolar spindle 1, Mps 1, TTK, inhibitor, diaminopyridine, peptide flip, cancer



Monopolar spindle 1 (Mps1), also known as TTK, is a dual-specificity protein kinase that is important for centrosome duplication, the spindle assembly checkpoint, and the maintenance of chromosomal stability.<sup>1–3</sup> Mps1 is activated during mitosis and highly expressed in cancer cells.<sup>4–7</sup> A recent report has shown that siRNA depletion of Mps1 resulted in aberrant mitoses and induction of apoptosis in breast cancer cells, which ultimately decreased the chance of survival. In contrast, there has been no significant increase in apoptosis in Mps1-depleted nonmalignant cells. Furthermore, Mps1 depletion by shRNA leads to apoptosis and reduced tumor volume in breast cancer xenograft models.<sup>7</sup> Such evidence points to Mps1 as a promising target in the development of anticancer therapeutics.

Only a few classes of Mps1 inhibitors have been reported.<sup>8–10</sup> For example, Nerviano Medical Sciences disclosed pyrimidine-based inhibitor **1** (NMS-P715), which shows antiproliferation effects over a large cancer cell line panel and inhibits tumor growth in A2780 ovary carcinoma and A375 melanoma xenograft models (Figure 1).<sup>8</sup>

c-Jun N-terminal kinase (JNK) inhibitors seem to be good templates for the design of novel Mps1 inhibitors. Bamborough

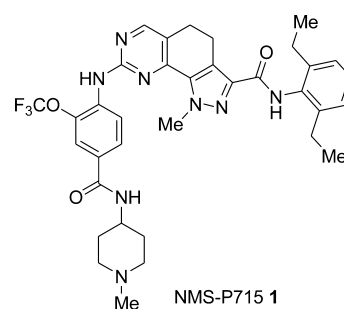


Figure 1. Structure of NMS-P715 (**1**).

et al. screened 577 compounds against 203 kinases, successfully analyzing them and creating a kinase structure–activity relationship (SAR) similarity tree (which is analogous to the kinome phylogenetic tree), using similarity matrices derived from their SAR data. According to the SAR similarity tree,

Received: April 7, 2012

Accepted: June 6, 2012

Published: June 6, 2012

Mps1 and JNK1 are grouped together, while they are in different sub-branches in the kinome phylogenetic tree.<sup>11</sup> Interestingly, despite sharing only 27% kinase domain sequence identity between Mps1 and JNK1, they possess SAR similarity. One possible explanation for this is that the gatekeeper residues between these kinases are conserved (Met). However, Met is a frequent gatekeeper residue<sup>12</sup> and thus using other specific ATP site-residues may make it possible to gain this similarity in addition to the gatekeeper residues. Indeed, JNK inhibitor SP600125 is a highly potent inhibitor of Mps1.<sup>13,14</sup> Although SP600125 is also known as a pan-kinase inhibitor, it has induced mitotic phenotypes in human cells consistent with Mps1 inhibition.<sup>3,15</sup> Taken together, it is likely that analogue synthesis and isosteric replacements of JNK inhibitors provide an effective method for identifying novel Mps1 inhibitors.

Abbott Laboratories has reported the development of aminopyridine-based JNK inhibitors (Figure 2).<sup>16,17</sup> Amino-

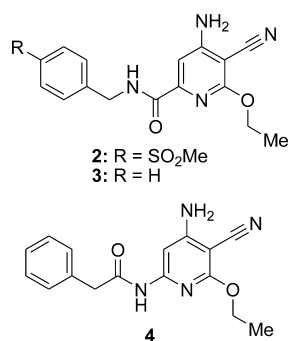


Figure 2. Abbott JNK inhibitors.

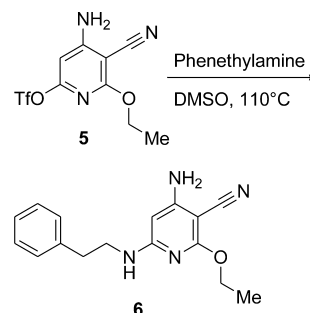
pyridine is an attractive scaffold for the lead compound because these analogues show a unique binding mode and excellent selectivity over 77 kinases. As a first step, we synthesized aminopyridine-based JNK inhibitor **2** and evaluated its inhibitory activity. As expected, **2** showed good potency for Mps1 (IC<sub>50</sub> = 568 nM), which encouraged us to initiate our medicinal chemistry efforts by utilizing the aminopyridine scaffold to discover a selective Mps1 inhibitor.

In this paper, we report on the design and synthesis of highly selective Mps1 inhibitors, which were found to reduce cancer cell proliferation and inhibit tumor growth in vivo. The X-ray structure of diaminopyridine **9** revealed that the Cys604 carbonyl group of the hinge region flips to form a hydrogen bond with the aniline NH group in **9**, which is likely contribute to the high selectivity of the optimized compound **12** for other kinases.

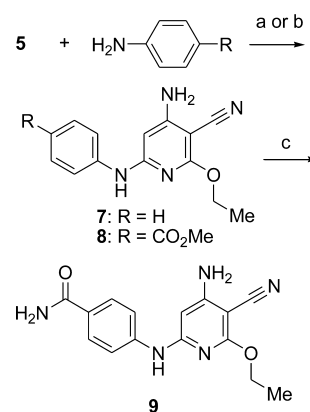
The synthesis of aminopyridine analogues is described in Scheme 1–3. Compound **6** was synthesized by heating compound **5** with phenethylamine (Scheme 1).<sup>17</sup> The synthesis of compounds **7** and **9** is illustrated in Scheme 2. Compound **5** was coupled with aniline and methyl 4-aminobenzoate using palladium-mediated amination to give compounds **7** and **8**, respectively. The hydrolysis of ester **8** followed by a HATU-mediated amide coupling gave compound **9**. Scheme 3 depicts the synthesis of compound **12**. Bromopyridine **10**<sup>16</sup> was reacted with *t*-butylamine in *N*-methylpyrrolidone (NMP) at 250 °C using a microwave reactor to give triaminopyridine **11**, which was then coupled with methyl 4-iodobenzoate followed by hydrolysis and amide coupling to give the final compound **12**.

We initially evaluated the SAR for compounds **2**–**4** as reported by Abbott (Table 1). Under our assay conditions,

### Scheme 1. Synthesis of **6**

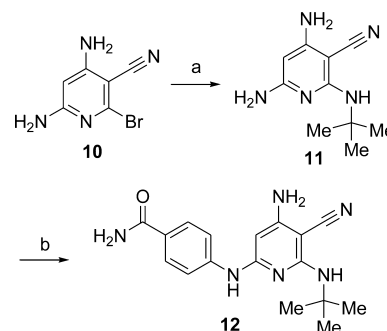


### Scheme 2. Synthesis of **9**<sup>a</sup>



<sup>a</sup>Reagents and conditions: (a) Et<sub>3</sub>N, DMSO, 180 °C (microwave). (b) Pd(OAc)<sub>2</sub>, BINAP, Cs<sub>2</sub>CO<sub>3</sub>, dioxane, reflux. (c) (i) Aqueous NaOH, DMSO, rt; (ii) HATU, Et<sub>3</sub>N, aqueous NH<sub>3</sub>, DMF, rt.

### Scheme 3. Synthesis of **12**<sup>a</sup>



<sup>a</sup>Reagents and conditions: (a) *t*-Butylamine, NMP, 250 °C (microwave). (b) (i) Methyl 4-iodobenzoate, Pd(OAc)<sub>2</sub>, xantphos, Cs<sub>2</sub>CO<sub>3</sub>, dioxane, reflux; (ii) aqueous NaOH, DMSO, rt; (iii) HATU, Et<sub>3</sub>N, aqueous NH<sub>3</sub>, DMF, rt.

Table 1. SAR of Aminopyridines

compd	IC <sub>50</sub> (nM)	
	Mps1	JNK1
2	568	4.7
3	529	350
4	4200	260
6	3970	>100000
7	228	1035
9	37	190
12	6.4	231

JNK1  $IC_{50}$  values of these compounds were comparable to the published values.<sup>16,17</sup> Introduction of a methylsulfonyl group was important for the JNK1 inhibitory activity, while such modification did not affect the Mps1 inhibitory activity as shown by compounds 2 and 3. Reversal of the amide connectivity resulted in compound 4 with an 8-fold loss in Mps1 activity, although 4 retained JNK1 activity. The X-ray crystal structures of Abbott's aminopyridine derivatives with JNK1 confirmed that the carbonyl oxygen at the 6-position of the pyridine forms a hydrogen bond with the Met111 NH group.<sup>16,17</sup> We therefore explored carbonyl surrogates for this 6-position. However, introduction of sulfonamides, ureas, and heterocycles (oxazoles and oxadiazoles) led to reduced Mps1 activity (data not shown). Interestingly, removal of the amide carbonyl group of compound 4 led to the phenethylamine analogue 6, which retained Mps1 activity, while JNK1 activity was completely abolished. Encouraged by this result, we investigated a number of amine analogues and discovered that aniline analogue 7 had a higher Mps1 potency than compounds 2 and 3. Finally, introduction of the amide group at the 4-position of the phenyl group in 7 gave rise to compound 9 with a 7-fold increase in Mps1 activity ( $IC_{50}$  = 37 nM).

Given the X-ray structure of aminopyridines with JNK1 reported by Abbott,<sup>16,17</sup> we were surprised to discover that the aniline analogues 7 and 9 exhibited Mps1 activity despite the absence of the carbonyl group at the pyridine 6-position. To elucidate the binding mode of aniline analogues, the X-ray structure of 9 with Mps1 was obtained at 2.40 Å resolution (Figure 3). To our surprise, the cocrystal structure in the ATP

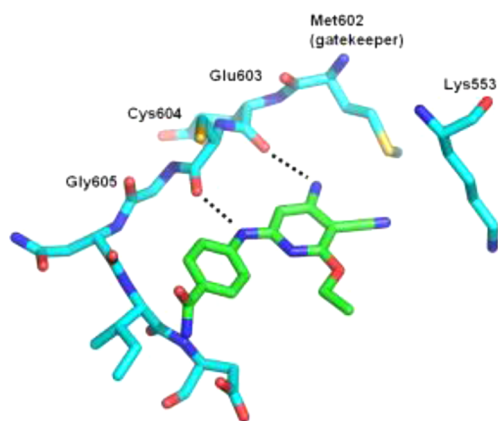


Figure 3. Crystal structure of 9 bound to Mps1 (PDB ID: 3VQU).

binding site of Mps1 revealed that the Cys604 carbonyl group of the hinge region flips to form a hydrogen bond with the aniline NH group in 9 (2.90 Å). The amino group at the 4-position of the pyridine in 9 also engages in a hydrogen bond with the carbonyl of Glu603 (2.94 Å). The pyridine lies in a hydrophobic pocket defined by Ile531, Val539, Leu654, and Ile663, and the cyano group on the pyridine ring points to the back pocket of the conserved Lys553. The phenyl ring also has van der Waals contact with Ile531 and Leu654 and is pointed toward the solvent. On the other hand, there are no clear interactions between the amide group on the phenyl ring and the protein in spite of the fact that this amide group contributes to a 6-fold increase in activity, as found for compounds 7 and 9.

Similar peptide flips at the hinge region have been observed in X-ray structures of quinazolinones,<sup>18,19</sup> pyridol-pyrimidines,<sup>18</sup> phthalazines,<sup>20,21</sup> pyridazinopyridinones,<sup>22</sup> PH-797804,<sup>23</sup> and VX-745<sup>24</sup> bound to p38 MAP kinase and a quinazoline bound to Mps1.<sup>25</sup> As illustrated in Figure 4a, the peptide flip in the p38α complexed with pyridol-pyrimidine 13 occurred at the main chain nitrogen between Met109 and Gly110. The G110A mutation of p38α resulted in a 14-fold decrease in activity, indicating that Gly110 makes the peptide flip more favorable. In our case, the peptide flip in Mps1 occurred at the main chain carbonyl of Cys604 (Figure 4b), and Gly605 next to Cys604 is thought to contribute to the peptide flip at Cys604.

Next, we turned our attention to the C2 side chain of the pyridine ring to further improve enzymatic activity and selectivity over JNK1. The crystal structure revealed that the C2 side chain of the ethyl ether lies in the ribose pocket that consists of hydrophobic residues Val539 and Ile663. Therefore, we examined a small set of hydrophobic substituents and found that substitution with a *t*-butylamino group (12) led to a 6-fold improvement in potency with a 36-fold selectivity for Mps1 over JNK1.

Once the highly potent Mps1 inhibitors 9 and 12 were identified, we examined the cellular effects of the compounds (Table 2). To investigate the cellular inhibition of Mps1, we

Table 2. Cellular Activity and Mouse PK Profile of 12

cellular activity		mouse PK po, 25 mg/kg		
pMps1 $IC_{50}$ (nM) <sup>a</sup>	A549 $IC_{50}$ (nM) <sup>b</sup>	$C_{max}$ (ng/ mL) <sup>c</sup>	$T_{max}$ (h) <sup>d</sup>	AUC <sub>po</sub> (ng h /mL) <sup>e</sup>
131	840	3542	0.25	6604

<sup>a</sup>Inhibition of autophosphorylation. <sup>b</sup>Cell viability in A549 cells at 72 h. <sup>c</sup>Maximum plasma concentration. <sup>d</sup>Time of maximum plasma concentration. <sup>e</sup>Area under the curve.

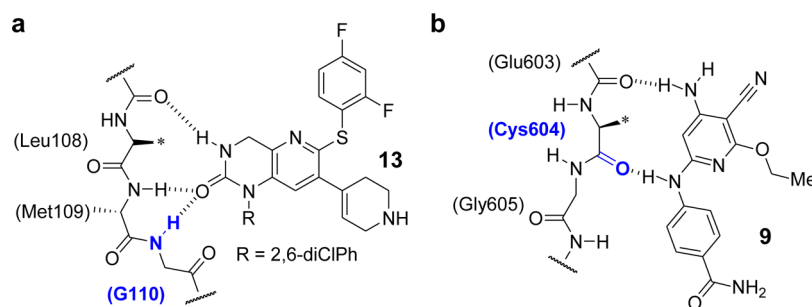
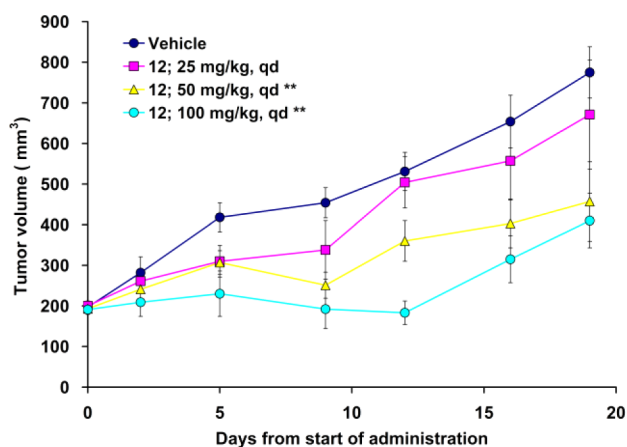


Figure 4. Comparison of the ligand-induced peptide flip in p38 Map kinase and Mps1. (a) Schematic diagram of compound 13 bound to p38 at the hinge region. (b) Compound 9 bound to Mps1 at the hinge region. The flipped residues are colored blue.

developed an autophosphorylation assay using a cell line that stably expresses FLAG-tagged Mps1 under the control of a tetracycline (Tet)-suppressible promoter. Compound **12** showed an  $IC_{50}$  value of 131 nM, while **9** showed weak inhibition (1.8  $\mu$ M) in this autophosphorylation assay. These antiproliferative activities were also examined in A549 lung carcinoma cell lines. Compounds **9** and **12** inhibited the growth of these cell lines with  $IC_{50}$  values of 9.5 and 0.84  $\mu$ M, respectively. The antiproliferative effects correlated with the cellular inhibition of Mps1.

To evaluate kinase selectivity, compound **12** was screened against a panel of 95 kinases. We found that **12** displayed an excellent selectivity profile in this panel, except for the Flt3 and Flt3 mutants (D835Y) (50 and 86% inhibition at 1  $\mu$ M, respectively; Supporting Information). This selectivity profile can be explained by the crystal structure of the enzyme and the inhibitor complex. Our compounds form hydrogen bonds with the flipped carbonyl of Cys604 next to Gly605 and the carbonyl of Glu603 at the hinge region in an unusual manner. Therefore, our Mps1 inhibitors do not have the ability to bind to the "usual" hinge regions of other kinases, which accounts for the excellent kinase selectivity of **12**.

The pharmacokinetic (PK) profile of **12** was studied using mice (Table 2). Compound **12** showed good PK properties with a  $C_{max}$  of 3542 ng/mL and AUC of 6604 ng h/mL at an oral dose of 25 mg/kg. Encouraged by these results, the in vivo efficacy of **12** was examined with the A549 xenograft model. Mice bearing xenografts were dosed orally once daily with an escalating dose from 25 to 100 mg/kg for 19 days. The results showed that **12** inhibited the growth of A549 cells in a dose-dependent manner (Figure 5). At a dose of 100 mg/kg, **12** exhibited 47% tumor growth inhibition without body weight loss.



**Figure 5.** Tumor growth efficacy of **12** in A549 xenograft model. Mice were dosed once daily for 19 days. Asterisks indicate a statistically significant difference from the vehicle-treated group based on the Dunnett's *t* test (\*\* $P \leq 0.01$ ).

In conclusion, potent and selective diaminopyridine-based Mps1 inhibitors have been successfully identified. X-ray crystallographic data indicate that the Cys604 carbonyl group of the hinge region flips to form a hydrogen bond with the aniline NH group at the 6-position of pyridine. The excellent kinase selectivity of the optimized compound **12** can be explained by the unusual peptide flip at the hinge region. The diaminopyridine scaffold should be a good template for more

advanced inhibitors of Mps1. Diaminopyridine **12** also exhibited good cellular activity and pharmacokinetic properties and was efficacious in the A549 lung cancer xenograft model. Additionally, **12** has good leadlike profiles: low MW (324), CLog *P* (2.8), and high LE (0.47). The selective Mps1 inhibitor **12** with in vivo efficacy could be used as a valuable tool for elucidating the biological functions in cancer therapy.

## ■ ASSOCIATED CONTENT

### Supporting Information

Experimental details for the synthesis and characterization of compounds **6**, **7**, **9**, and **12**; details of Mps1 enzyme inhibition, cell proliferation, autophosphorylation, and in vivo antitumor assays; crystallographic methods for the crystal structure of compound **9**; and kinase selectivity data for compound **12**. This material is available free of charge via the Internet at <http://pubs.acs.org>.

### Accession Codes

PDB ID: 3VQU (Figure 3 crystal structure).

## ■ AUTHOR INFORMATION

### Corresponding Author

\*Tel: +81(6)6331 8081. Fax: +81(6)6332 6385. E-mail: [ken-ichi.kusakabe@shionogi.co.jp](mailto:ken-ichi.kusakabe@shionogi.co.jp).

### Notes

The authors declare no competing financial interest.

## ■ ACKNOWLEDGMENTS

We thank Natsuki Ishizuka, Kazuya Okamoto, and Masahiko Huijoka for their synthetic support and Rikio Ikenishi and Yumiko Takagi for the elemental analysis. K.K. also acknowledges Robert Hall for his assistance in preparing this manuscript. We gratefully thank Kenji Abe, Yoshiyuki Matsuo, Hirosato Kondo, and Kohji Hanasaki for their helpful advice and suggestions during the course of this research.

## ■ ABBREVIATIONS

BINAP, 2,2'-bis(diphenylphosphino)-1,1'-binaphthyl; DMF, *N,N*-dimethylformamide; DMSO, dimethyl sulfoxide; Et<sub>3</sub>N, triethylamine; JNK, c-Jun N-terminal kinase; Mps1, monopolar spindle 1; NMP, *N*-methylpyrrolidone; SAR, structure–activity relationship; Tet, tetracycline, Pd(OAc)<sub>2</sub>, palladium(II) acetate; Xantphos, 4,5-bis(diphenylphosphino)-9,9-dimethylxanthene

## ■ REFERENCES

- (1) Fisk, H. A.; Mattison, C. P.; Winey, M. Human Mps1 protein kinase is required for centrosome duplication and normal mitotic progression. *Proc. Natl. Acad. Sci. U.S.A.* **2003**, *100*, 14875–14880.
- (2) Stucke, V. M.; Sillje, H. H. W.; Arnaud, L.; Nigg, E. A. Human Mps1 kinase is required for the spindle assembly checkpoint but not for centrosome duplication. *EMBO J.* **2002**, *21*, 1723–1732.
- (3) Jelluma, N.; Brenkman, A. B.; van den Broek, N. J. F.; Crujisen, C. W. A.; van Osch, M. H. J.; Lens, S. M. A.; Medema, R. H.; Kops, Geert, J. P. L. Mps1 phosphorylates borealin to control aurora B activity and chromosome alignment. *Cell (Cambridge, MA, U. S.)* **2008**, *132*, 233–246.
- (4) Saito-Hisaminato, A.; Katagiri, T.; Kakiuchi, S.; Nakamura, T.; Tsunoda, T.; Nakamura, Y. Genome-wide profiling of gene expression in 29 normal human tissues with a cDNA microarray. *DNA Res.* **2002**, *9*, 35–45.
- (5) Kikuchi, T.; Daigo, Y.; Katagiri, T.; Tsunoda, T.; Okada, K.; Kakiuchi, S.; Zembutsu, H.; Furukawa, Y.; Kawamura, M.; Kobayashi, K.; Imai, K.; Nakamura, Y. Expression profiles of non-small cell lung



cancers on cDNA microarrays: Identification of genes for prediction of lymph-node metastasis and sensitivity to anti-cancer drugs. *Oncogene* **2003**, *22*, 2192–2205.

(6) Yamabuki, T.; Daigo, Y.; Kato, T.; Hayama, S.; Tsunoda, T.; Miyamoto, M.; Ito, T.; Fujita, M.; Hosokawa, M.; Kondo, S.; Nakamura, Y. Genome-wide gene expression profile analysis of esophageal squamous cell carcinomas. *Int. J. Oncol.* **2006**, *28*, 1375–1384.

(7) Daniel, J.; Coulter, J.; Woo, J.-H.; Wilsbach, K.; Gabrielson, E. High levels of the Mps1 checkpoint protein are protective of aneuploidy in breast cancer cells. *Proc. Natl. Acad. Sci. U.S.A.* **2011**, *108*, 5384–5389.

(8) Colombo, R.; Caldarelli, M.; Mennecozzi, M.; Giorgini, M. L.; Sola, F.; Cappella, P.; Perrera, C.; Depaolini, S. R.; Rusconi, L.; Cucchi, U.; Avanzi, N.; Bertrand, J. A.; Bossi, R. T.; Pesenti, E.; Galvani, A.; Isacchi, A.; Colotta, F.; Donati, D.; Moll, J. Targeting the mitotic checkpoint for cancer therapy with NMS-P715, an inhibitor of MPS1 kinase. *Cancer Res.* **2010**, *70*, 10255–10264.

(9) Caldarelli, M.; Angiolini, M.; Disingrini, T.; Donati, D.; Guanci, M.; Nuvoloni, S.; Poster, H.; Quartieri, F.; Silvagni, M.; Colombo, R. Synthesis and SAR of new pyrazolo[4,3-h]quinazoline-3-carboxamide derivatives as potent and selective MPS1 kinase inhibitors. *Bioorg. Med. Chem. Lett.* **2011**, *21*, 4507–4511.

(10) Tardif, K. D.; Rogers, A.; Cassiano, J.; Roth, B. L.; Cimbor, D. M.; McKinnon, R.; Peterson, A.; Douce, T. B.; Robinson, R.; Dorweiler, I.; Davis, T.; Hess, M. A.; Ostanin, K.; Papac, D. I.; Baichwal, V.; McAlexander, L.; Willardsen, J. A.; Saunders, M.; Christophe, H.; Kumar, D. V.; Wettstein, D. A.; Carlson, R. O.; Williams, B. L. Characterization of the cellular and antitumor effects of MPI-0479605, a small-molecule inhibitor of the mitotic kinase Mps1. *Mol. Cancer Ther.* **2011**, *10*, 2267–2275.

(11) Bamborough, P.; Drewry, D.; Harper, G.; Smith, G. K.; Schneider, K. Assessment of chemical coverage of kinome space and its implications for kinase drug discovery. *J. Med. Chem.* **2008**, *51*, 7898–7914.

(12) Zuccotto, F.; Ardini, E.; Casale, E.; Angiolini, M. Through the “gatekeeper door”: Exploiting the active kinase conformation. *J. Med. Chem.* **2010**, *53*, 2681–2694.

(13) Chu, M. L. H.; Chavas, L. M. G.; Douglas, K. T.; Eysers, P. A.; Tabernero, L. Crystal structure of the catalytic domain of the mitotic checkpoint kinase Mps1 in complex with SP600125. *J. Biol. Chem.* **2008**, *283*, 21495–21500.

(14) Fabian, M. A.; Biggs, W. H.; Treiber, D. K.; Atteridge, C. E.; Azimioara, M. D.; Benedetti, M. G.; Carter, T. A.; Ciceri, P.; Edeen, P. T.; Floyd, M.; Ford, J. M.; Galvin, M.; Gerlach, J. L.; Grotzfeld, R. M.; Herrgard, S.; Insko, D. E.; Insko, M. A.; Lai, A. G.; Lelias, J.-M.; Mehta, S. A.; Milanov, Z. V.; Velasco, A. M.; Wodicka, L. M.; Patel, H. K.; Zarrinkar, P. P.; Lockhart, D. J. A small molecule-kinase interaction map for clinical kinase inhibitors. *Nat. Biotechnol.* **2005**, *23*, 329–336.

(15) Schmidt, M.; Budirahardja, Y.; Klompmaier, R.; Medema, R. H. Ablation of the spindle assembly checkpoint by a compound targeting Mps1. *EMBO Rep.* **2005**, *6*, 866–872.

(16) Szczepankiewicz, B. G.; Kosogof, C.; Nelson, L. T. J.; Liu, G.; Liu, B.; Zhao, H.; Serby, M. D.; Xin, Z.; Liu, M.; Gum, R. J.; Haasch, D. L.; Wang, S.; Clampit, J. E.; Johnson, E. F.; Lubben, T. H.; Stashko, M. A.; Olejniczak, E. T.; Sun, C.; Dorwin, S. A.; Haskins, K.; Abad-Zapatero, C.; Fry, E. H.; Hutchins, C. W.; Sham, H. L.; Rondinone, C. M.; Trevillyan, J. M. Aminopyridine-based c-Jun N-terminal kinase inhibitors with cellular activity and minimal cross-kinase activity. *J. Med. Chem.* **2006**, *49*, 3563–3580.

(17) Zhao, H.; Serby, M. D.; Xin, Z.; Szczepankiewicz, B. G.; Liu, M.; Kosogof, C.; Liu, B.; Nelson, L. T. J.; Johnson, E. F.; Wang, S.; Pederson, T.; Gum, R. J.; Clampit, J. E.; Haasch, D. L.; Abad-Zapatero, C.; Fry, Elizabeth, H.; Rondinone, C.; Trevillyan, J. M.; Sham, H. L.; Liu, G. Discovery of potent, highly selective, and orally bioavailable pyridine carboxamide c-Jun NH2-terminal kinase inhibitors. *J. Med. Chem.* **2006**, *49*, 4455–4458.

(18) Fitzgerald, C. E.; Patel, S. B.; Becker, J. W.; Cameron, P. M.; Zaller, D.; Pikounis, V. B.; O’Keefe, S. J.; Scapin, G. Structural basis for

p38 $\alpha$  MAP kinase quinazolinone and pyridol-pyrimidine inhibitor specificity. *Nat. Struct. Biol.* **2003**, *10*, 764–769.

(19) Stelmach, J. E.; Liu, L.; Patel, S. B.; Pivnichny, J. V.; Scapin, G.; Singh, S.; Hop, C. E. C. A.; Wang, Z.; Strauss, J. R.; Cameron, P. M.; Nichols, E. A.; O’Keefe, S. J.; O’Neill, E. A.; Schmatz, D. M.; Schwartz, C. D.; Thompson, C. M.; Zaller, D. M.; Doherty, J. B. Design and synthesis of potent, orally bioavailable dihydroquinazolinone inhibitors of p38 MAP kinase. *Bioorg. Med. Chem. Lett.* **2003**, *13*, 277–280.

(20) Herberich, B.; Cao, G.-Q.; Chakrabarti, P. P.; Falsey, J. R.; Pettus, L.; Rzasa, R. M.; Reed, A. B.; Reichelt, A.; Sham, K.; Thaman, M.; Wurz, R. P.; Xu, S.; Zhang, D.; Hsieh, F.; Lee, M. R.; Syed, R.; Li, V.; Grosfeld, D.; Plant, M. H.; Henkle, B.; Sherman, L.; Middleton, S.; Wong, L. M.; Tasker, A. S. Discovery of highly selective and potent p38 inhibitors based on a phthalazine scaffold. *J. Med. Chem.* **2008**, *51*, 6271–6279.

(21) Pettus, L. H.; Xu, S.; Cao, G.-Q.; Chakrabarti, P. P.; Rzasa, R. M.; Sham, K.; Wurz, R. P.; Zhang, D.; Middleton, S.; Henkle, B.; Plant, M. H.; Saris, C. J. M.; Sherman, L.; Wong, L. M.; Powers, D. A.; Tudor, Y.; Yu, V.; Lee, M. R.; Syed, R.; Hsieh, F.; Tasker, A. S. 3-Amino-7-phthalazinylbenzoisoxazoles as a novel class of potent, selective, and orally available inhibitors of p38 $\alpha$  mitogen-activated protein kinase. *J. Med. Chem.* **2008**, *51*, 6280–6292.

(22) Wu, B.; Wang, H.-L.; Pettus, L.; Wurz, R. P.; Doherty, E. M.; Henkle, B.; McBride, H. J.; Saris, C. J. M.; Wong, L. M.; Plant, M. H.; Sherman, L.; Lee, M. R.; Hsieh, F.; Tasker, A. S. Discovery of pyridazinopyridinones as potent and selective p38 mitogen-activated protein kinase inhibitors. *J. Med. Chem.* **2010**, *53*, 6398–6411.

(23) Xing, L.; Shieh, H. S.; Selness, S. R.; Devraj, R. V.; Walker, J. K.; Devadas, B.; Hope, H. R.; Compton, R. P.; Schindler, J. F.; Hirsch, J. L.; Benson, A. G.; Kurumbail, R. G.; Stegeman, R. A.; Williams, J. M.; Broadus, R. M.; Walden, Z.; Monahan, J. B. Structural bioinformatics-based prediction of exceptional selectivity of p38 MAP kinase inhibitor PH-797804. *Biochemistry* **2009**, *48*, 6402–6411.

(24) Duffy, J. P.; Harrington, E. M.; Salituro, F. G.; Cochran, J. E.; Green, J.; Gao, H.; Bemis, G. W.; Evindar, G.; Galullo, V. P.; Ford, P. J.; Germann, U. A.; Wilson, K. P.; Bellon, S. F.; Chen, G.; Taslimi, P.; Jones, P.; Huang, C.; Pazhanisamy, S.; Wang, Y.-M.; Murcko, M. A.; Su, Michael, S. S. The discovery of VX-745: A novel and selective p38 $\alpha$  kinase inhibitor. *ACS Med. Chem. Lett.* **2011**, *2*, 758–763.

(25) Chu, M. L. H.; Lang, Z.; Chavas, L. M. G.; Neres, J.; Fedorova, O. S.; Tabernero, L.; Cherry, M.; Williams, D. H.; Douglas, K. T.; Eysers, P. A. Biophysical and X-ray crystallographic analysis of Mps1 kinase inhibitor complexes. *Biochemistry* **2010**, *49*, 1689–1701.